Improving watermark resistance against removal attacks using orthogonal wavelet adaptation

Jan Stolarek and Piotr Lipiński

Institute of Information Technology
Technical University of Lodz
Poland
jan.stolarek@p.lodz.pl, piotr.lipinski@p.lodz.pl

Abstract. This paper proposes a new approach for enhancing the robustness of wavelet-based image watermarking algorithms. The method adjusts wavelet used in the process of image watermarking in order to maximize resistance against image processing operations. Effectiveness of the approach is demonstrated using blind multiplicative watermarking algorithm, but it can easily be generalized to all wavelet-based watermarking algorithms. Presented results demonstrate that wavelets generated using proposed approach outperform other wavelet bases commonly used in image watermarking in terms of robustness to removal attacks.

1 Introduction

Discrete Wavelet Transform (DWT) is widely applied in the field of digital image watermarking. Despite the popularity and proliferation of DWT-based watermarking algorithms, the following aspects attract surprisingly little attention: the influence of DWT filter coefficients on watermarked image fidelity and the influence of DWT filter coefficients on watermark robustness against attacks. Although the problem of choosing the optimal wavelet has been noticed by some authors [7, 12], so far there have been no attempts to optimize the wavelet in order to increase either the watermarked image fidelity or attack resistance of the watermark. Huang and Jiang in [8] notice the influence of wavelet filter coefficients on watermarking fidelity, but they do not optimize it. Instead, they use wavelet filter parameters as a private key to increase security of the watermark. A similar approach is presented in [2] for two-dimensional case.

The algorithm for improving the watermarked image fidelity and watermark separability by wavelet adaptation has already been presented in [11]. In this paper we modify that algorithm in order to increase the watermarking robustness against removal attacks [16] while maintaining constant image fidelity. It will be demonstrated that the presented algorithm adapts the wavelet to a cover image and a watermark signal. Image fidelity assessment using the MSE measure was replaced by the Wang-Bovik Index [17].

2 Orthogonal wavelet filter parametrization

Orthogonal wavelet transform is implemented by an orthonormal filter bank, each of the filters having impulse response of even length L. In the case of wavelets, $L/2+1$ degrees of freedom are bound by the theoretical conditions imposed on the filters. The remaining $L/2-1$ degrees of freedom can be manipulated to adapt the properties of the filter. In order to effectively synthesize wavelets a filter parametrization must be defined. In this paper, parametrization based on the lattice filter [14] is used, following the description given in [18]. Basic operations of the lattice filter are orthogonal 2×2 rotations, which ensure both orthogonality of the structure and perfect reconstruction of the signal. For a filter of length L, $L/2$ orthogonal rotations have to be used. Fig.1 shows an example of a filter implementing 4-tap transform ($G(z)$ and $H(z)$ are the low-pass and high-pass filter outputs respectively). To ensure that wavelet implemented by the lattice filter has zero mean, the sum of all rotation angles in the structure must equal $-45°$ [13]:

$$\sum_{k=0}^{L/2} \alpha_k = -45^\circ \ , \tag{1}$$

where α_k are the angles of the orthogonal rotations. In order to ensure that this condition is always fulfilled, the following substitution can be used [13]:

$$\begin{aligned} &\alpha_1 = \vartheta - \varphi_1 \ , \\ &\alpha_i = (-1)^i(\varphi_{i-1} + \varphi_i) \ , \text{ for } i = 2, \ldots, \frac{L}{2} - 1 \ , \\ &\alpha_{\frac{L}{2}} = \varphi_{\frac{L}{2}-1} \ . \end{aligned} \tag{2}$$

The above shows that wavelets parametrized using the lattice filter are defined by a set of $L/2-1$ rotation angles φ_k.

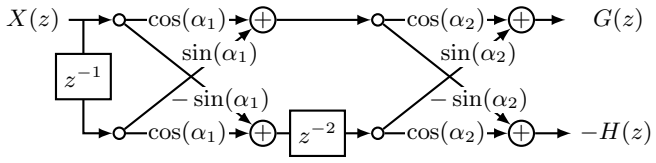

Fig. 1: Lattice filter implementing a 4-tap wavelet transform.

3 Image watermarking in the wavelet transform domain

Fig.2a shows the generic scheme of digital image watermark embedding in the wavelet transform domain. The image to be watermarked is decomposed using

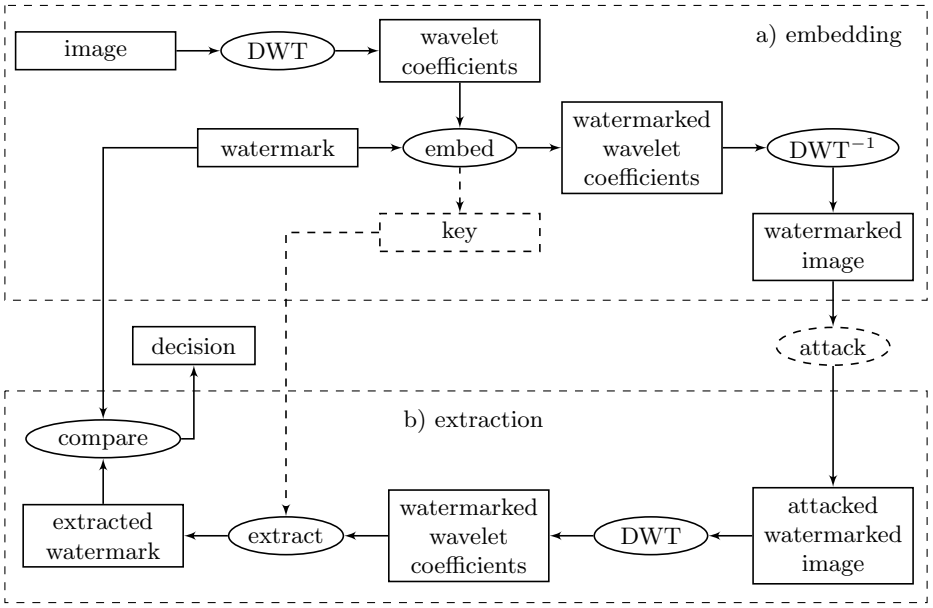

Fig. 2: Generic scheme of watermark embedding and blind extraction in the wavelet transform domain. Rectangles represent data, elipses represent algorithms.

from 3 to 5 levels of DWT. Watermark sequence is then embedded in the wavelet coefficients. Some embedding algorithms return supplementary data – a *key* – that is essential to successfully extract the watermark. The image is reconstructed using the inverse wavelet transform (denoted as DWT^{-1} in Fig.2a) and it is released to the public where it may be subjected to attacks, i.e. operations – deliberate or not – that make the watermark extraction and identification more difficult. To check for watermark presence the presumably watermarked and/or possibly attacked image has to be decomposed using the same number of DWT levels as was used for watermark embedding. Watermark is then extracted from the wavelet coefficients (using the optional key, if necessary) and compared with the embedded one. Schemes that do not require knowledge of the original image are called *blind*. It must be noted that this generic scheme may differ in details for particular embedding algorithms.

The improvement method presented in this paper is a general one and can be used to enhance any wavelet-based watermarking algorithm. For demonstration purposes the simplest blind multiplicative watermarking method was used, in which the watermark $\mathbf{w}$ is a sequence of N random numbers from set $\{-1, 1\}$ and the embedding formula is

$$\mathbf{c}^{(w)} = \mathbf{c} + \kappa \cdot |\mathbf{c}| \cdot \mathbf{w} \ , \tag{3}$$

where $\mathbf{c}$ are the N largest wavelet coefficients selected from the highest level detail subbands (see Fig.3), κ is the embedding strength, $|\cdot|$ denotes the absolute

value, $\mathbf{w}$ is the watermark sequence and $\mathbf{c}^{(w)}$ are the watermarked wavelet coefficients. Operations on the vectors in (3) are performed element-wise. Locations of the watermarked coefficients $\mathbf{c}^{(w)}$ have to be stored, since they are required in the process of watermark extraction – these locations play the role of the key (see Fig.2). To detect the presence of the watermark, normalized correlation between the embedded watermark and the presumably watermarked coefficients is calculated using the formula

$$C = \frac{1}{N-1} \sum_{i=1}^{N} \frac{(c_i^{(w)} - \overline{c^{(w)}})(w_i - \overline{\mathbf{w}})}{\sigma_c \sigma_w} \quad , \tag{4}$$

where $c_i^{(w)}$ are the presumed watermarked coefficients, $\overline{c^{(w)}}$ is the mean value of the watermarked coefficients, w_i are the embedded watermark values, $\overline{\mathbf{w}}$ is the mean value of the embedded watermark, σ_c and σ_w are standard deviations of watermarked coefficients and the watermark respectively.

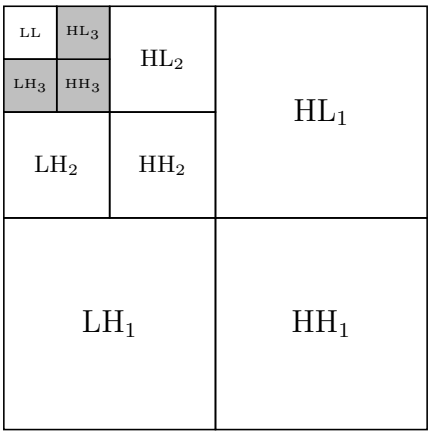

Fig. 3: Wavelet decomposition of an image. Watermark is embedded in the third level detail subbands, corresponding to middle frequencies (in gray).

In the digital image watermarking there are three main requirements, that determine whether the watermarking process is effective:

- Fidelity: watermarking process must not degrade the quality of the watermarked image.
- Separability: the extracted watermark must have significantly greater normalized correlation with the embedded watermark than with random watermarks. This ensures faultless watermark detection and distinction.
- Attack resistance: watermark separability must be maintained despite image manipulations (unless the image is damaged beyond usability).

It has already been demonstrated [11] that the mother wavelet used for image decomposition can be adjusted to the image, the watermark and the watermarking algorithm in order to improve separability and fidelity. In this paper we modified that system to maximize watermark resistance against image processing operations and maintain constant fidelity of the watermarked image.

4 Watermarked image fidelity

We assess the fidelity of the watermarked image using the Wang-Bovik Index (WBI) [17], which takes into account the loss of correlation, luminance distortion and contrast distortion, thus offering a better image quality estimation than the widely used MSE. The original WBI is calculated by using the moving window approach. For each window the index between original image X and watermarked image Y is calculated using the following formula:

$$Q_m = \frac{4\sigma_{xy}\overline{x}\overline{y}}{(\sigma_x^2 + \sigma_y^2)[(\overline{x})^2 + (\overline{y})^2]} \ , \tag{5}$$

where $\overline{x}$ and $\overline{y}$ are mean values of pixels in a window, σ_x^2 and σ_y^2 are the variances, σ_{xy} is given as

$$\sigma_{xy} = \frac{1}{N-1}\sum_{i=1}^{N}(x_i - \overline{x})(y_i - \overline{y}) \ , \tag{6}$$

where x_i and y_i denote pixels of non-watermarked and watermarked image window respectively and N denotes the number of pixels in a single window. The moving window approach creates a map of distortions, where each $Q_m \in [-1, 1]$. We found that converting this map to a single value describing quality of an image – which is required if the constant distortion rate is to be maintained – is problematic. We achieved the best result by dropping the moving window approach and calculating WBI once for the whole image instead. To ensure that the distortion of the watermarked image was constant for every image, watermark and wavelet, the embedding strength κ in (3) was adjusted using Matlab's `fmincon` function.

5 Improving watermark attack resistance

In commonly used DWT-based watermarking algorithms wavelet basis used for image decomposition and reconstruction is chosen arbitrarily. As a result the wavelets used in watermark embedding are suboptimal for a given cover image, watermark, embedding algorithm and attacks. In this paper we used evolutionary approach to synthesize wavelet basis that adapts to the cover image, watermark and embedding algorithm and also provides better robustness against attacks than already existing wavelets. Simple Genetic Algorithm (SGA) combined with Evolution Strategies was applied. SGA maintains a population of possible solutions called *individuals*. Each individual represents a wavelet filter parametrized

using the lattice structure. Therefore, the filter of length L was represented as a set of $\frac{L}{2} - 1$ binary coded φ_i angles. Watermark resistance against selected attacks (e.g. JPEG compression, median filtering, noise contamination etc.) was increased by carrying out the attacks independently on the watermarked image. For each attack the watermark extraction was performed and partial fitnesses based on separability of the watermark were assigned to an individual:

$$F_j(k) = \min_{i \in \{1,\ldots,M\}} (C_e^{(k)} - C_r^{(i,k)}) \ , \tag{7}$$

where $k \in \{1, \ldots, K\}$ is index of the attack and $k = 0$ denotes no attack, j is the index of an individual, $C_e^{(k)}$ is the normalized correlation between the extracted watermark and the embedded watermark for k-th attack and $C_r^{(i,k)}$ is the normalized correlation between the extracted watermark and the i-th random watermark and k-th attack. M denotes the number of random watermarks. The smallest difference between the correlations was selected as individual's fitness. Since $C_e^{(k)}, C_r^{(i,k)} \in [-1, 1]$, then $F_j(k) \in [-2, 2]$. Tournament selection was used and therefore normalization of $F_j(k)$ to ensure that it was greater than zero was avoided. Introducing (7) created selection pressure that promoted individuals maximizing the separability despite the image distortion introduced by the attack.

The lowest partial fitness was selected as the total fitness of an individual:

$$F_j = \min_{k \in \{0,\ldots,K\}} \{F_j(k)\} \ . \tag{8}$$

This approach ensured that synthesized wavelets offered high resistance to all of the performed attacks. Wavelets that failed to meet the high robustness requirement against at least one of the attacks were assigned low fitness value, which eventually led to their elimination in the genetic algorithm. The scheme of the fitness evaluation algorithm is given in Fig.4.

6 Experimental results

For our experiments, we selected 20 images from the USC-SIPI Image Database (including textures and well-known images like Lena, Barbara, Baboon, Airplane, Boat, Lake etc.). A watermark $\mathbf{w}$ consisting of 512 random values in $\{-1, 1\}$ was embedded in the third level detail subbands and the acceptable perceptual image distortion rate was selected to WBI = 0.996. Separability given by (7) was used to characterize the robustness of the watermarking algorithm. 1000 randomly generated watermarks were used for calculating the separability. Removal attacks contained JPEG compression, median filtering, low-pass filtering and scaling (the image was scaled down to 40% of original size and then rescaled to original size).

The proposed algorithm was used to synthesize the optimal wavelet filter for every selected image. Orthogonal wavelets of length 4, 6, 8, 12 and 20 taps were synthesized. Due to lack of space, detailed results are presented only for

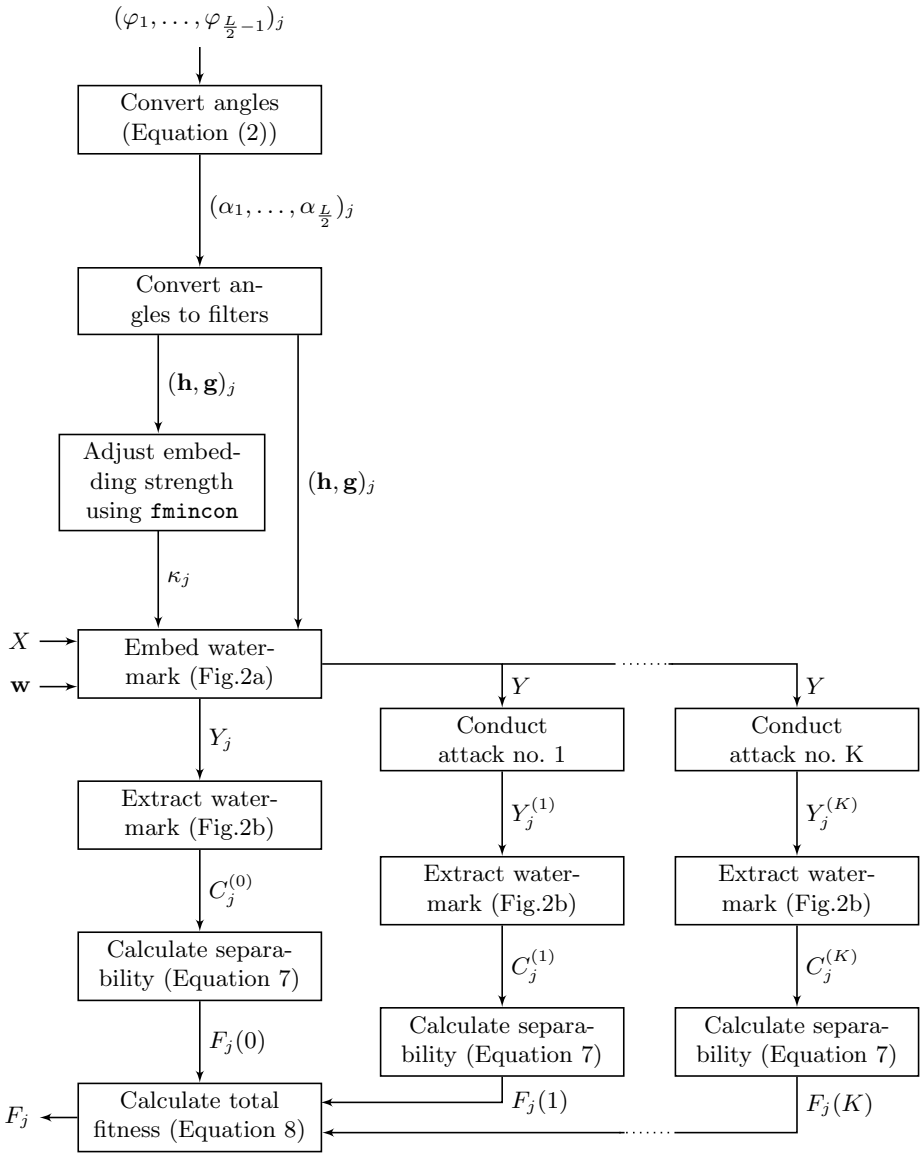

Fig. 4: Fitness evaluation scheme. X represents the original image, Y represents the image watermarked with $\mathbf{w}$, j is na index of an indvidual in a population.

Table 1: Comparison of separability values for adaptive wavelets and commonly used wavelets for Boat test image. Adaptive wavelet denoted with bold font, biorthogonal wavelets denoted with oblique font.

no attack		JPEG compression		median filter		low-pass filter		scaling	
A6	0.327	**A6**	0.302	**A6**	0.311	**A6**	0.315	**A6**	0.311
A12	0.311	**A8**	0.279	**A8**	0.275	**A20**	0.272	**A8**	0.268
A8	0.306	**A4**	0.268	**A20**	0.270	**A8**	0.268	**A4**	0.263
A4	0.291	**A20**	0.265	**A4**	0.262	**A4**	0.258	**A20**	0.258
A20	0.281	**A12**	0.233	**A12**	0.251	**A12**	0.249	**A12**	0.246
C6	0.273	C12	0.230	C6	0.242	S12	0.242	C6	0.239
D4	0.265	*V3*	0.226	S12	0.241	C6	0.241	D4	0.226
S12	0.259	S12	0.224	C12	0.237	C12	0.238	C12	0.214
Ha	0.251	C6	0.224	*V2*	0.231	*V6*	0.235	*V2*	0.205
C12	0.250	*V5*	0.217	*V6*	0.226	*V2*	0.230	*V3*	0.204
V2	0.244	*V6*	0.217	D4	0.220	*V3*	0.218	D8	0.202
V6	0.242	Ha	0.210	*V3*	0.220	D4	0.217	*V6*	0.197
V5	0.233	*V2*	0.188	D8	0.214	D8	0.215	*V5*	0.197
V3	0.231	D8	0.180	*V5*	0.213	*CDF*	0.210	S8	0.193
D8	0.231	*CDF*	0.176	*CDF*	0.210	*V5*	0.201	S12	0.190
CDF	0.214	C18	0.175	Ha	0.198	*An*	0.185	C18	0.179
An	0.209	D4	0.172	*An*	0.189	C18	0.184	*Od*	0.178
LG	0.203	S10	0.165	S8	0.187	S8	0.184	*An*	0.172
S8	0.201	S8	0.164	C18	0.185	Ha	0.178	*LG*	0.158
C18	0.199	*V4*	0.155	*Od*	0.174	*Od*	0.175	*CDF*	0.157
Od	0.189	*An*	0.153	*LG*	0.164	*LG*	0.172	Ha	0.153
S10	0.183	*LG*	0.150	S10	0.163	S10	0.168	D6	0.150
V4	0.177	*Od*	0.146	*V4*	0.155	*V4*	0.160	S10	0.141
D6	0.173	D6	0.138	D6	0.148	D6	0.144	*V4*	0.119

two example images: one photo (Boat) and one texture (Fig.5b). The robustness of adaptive wavelets (denoted as **A**) was compared with other wavelets known from the literature: orthogonal Haar (Ha), Daubechies (D4, D6, D8), Symlet (S4, S6, S8) and Coiflet (C6, C12, C18) wavelets [5] and the biorthogonal CDF 9/7 (*CDF*) [3], LeGall 5/3 (*LG*) [9], Antonini 9/7 (*An*) [1], Odegard (*Od*) [6], Villasenor 13/11 (*V2*), 6/10 (*V3*), 5/3 (*V4*), 2/6 (*V5*), 9/3 (*V6*) [15] wavelets. Each of these wavelets was used to embed the watermark in an image and the separability – with and without the attacks – was calculated. Tables 1 and 2 present separability values for all of the above mentioned wavelets. The first column contains separability for watermarked, unattacked image; the second column: separability for JPEG attack; the third column: separability for median attack; the fourth column: separability for low-pass filter; the fifth column: separability for scaling attack.

The results show that in each case the adaptive wavelets outperform wavelets proposed in the literature. Furthermore, no non-adaptive wavelet could be considered the best, as they perform differently depending on the conducted attack

Table 2: Comparison of separability values for adaptive wavelets and commonly used wavelets for texture test image. Adaptive wavelet denoted with bold font, biorthogonal wavelets denoted with oblique font.

no attack		JPEG compression		median filter		low-pass filter		scaling	
A4	0.717	**A8**	0.623	**A4**	0.679	**A4**	0.653	**A6**	0.517
A20	0.699	**A4**	0.575	**A6**	0.642	**A12**	0.619	**A12**	0.492
A8	0.685	**A6**	0.568	**A20**	0.635	**A6**	0.614	**A4**	0.492
A6	0.663	**A12**	0.547	**A8**	0.634	**A20**	0.607	**A8**	0.490
A12	0.649	**A20**	0.546	**A12**	0.620	**A8**	0.605	**A20**	0.439
C6	0.603	C6	0.539	C6	0.577	C6	0.552	C6	0.418
V4	0.532	*V4*	0.408	*V4*	0.508	*V4*	0.510	*V4*	0.362
LG	0.516	*An*	0.405	*LG*	0.493	*LG*	0.496	*CDF*	0.359
An	0.490	*LG*	0.398	*An*	0.457	*An*	0.470	*LG*	0.346
CDF	0.413	C12	0.327	*CDF*	0.395	*CDF*	0.404	*Od*	0.345
C12	0.384	*CDF*	0.317	C12	0.358	C12	0.363	*An*	0.344
Od	0.341	*Od*	0.287	*Od*	0.323	*Od*	0.340	C12	0.321
V6	0.328	*V6*	0.239	*V6*	0.306	*V6*	0.324	*V6*	0.263
D6	0.267	D6	0.226	D6	0.241	D6	0.252	D6	0.235
V2	0.248	C18	0.213	*V2*	0.231	*V2*	0.245	*V2*	0.228
C18	0.239	*V2*	0.195	C18	0.219	C18	0.217	C18	0.199
D4	0.229	S8	0.147	D4	0.195	D4	0.192	D4	0.195
S8	0.173	D4	0.143	S8	0.153	S8	0.167	S8	0.157
S10	0.122	S10	0.100	S10	0.108	S10	0.110	S12	0.147
S12	0.122	S12	0.096	S12	0.103	S12	0.105	S10	0.103
Ha	0.093	Ha	0.075	Ha	0.069	D8	0.068	D8	0.081
D8	0.080	*V5*	0.073	*V5*	0.067	*V5*	0.065	Ha	0.053
V5	0.074	*V3*	0.055	D8	0.064	*V3*	0.056	*V3*	0.049
V3	0.056	D8	0.051	*V3*	0.045	Ha	0.050	*V5*	0.039

even though the same image and watermark are used. This confirms the observations made by Dietze and Jassim [7] that no single wavelet can be regarded as optimal in terms of robustness. The proposed algorithm overcomes this limitation by adapting to the image, the watermark and the watermarking algorithm. This can be demonstrated by embedding the watermark in the Boat image using adaptive wavelets synthesized for Lena image. The result of such an experiment is shown in Table 3. It can be clearly noticed that the performance of adaptive wavelets has degraded significantly. For each image the synthesized wavelet is different. Fig.6a and Fig.6b show example scaling functions synthesized for two of the test images. Function in Fig.6b resembles Coiflet 6 wavelet and indeed the Coiflet 6 wavelet performs better than other non-adaptive wavelets for the example texture image. Tables 1 and 2 allow also to conclude that the algorithm works for different classes of images (natural and textures).

Table 3: Comparison of separability values for adaptive wavelets synthesized for Lena image and used to embed the watermark in Boat image. Adaptive wavelet denoted with bold font, biorthogonal wavelets denoted with oblique font.

no attack		JPEG compression		median filter		low-pass filter		scaling	
C6	0.273	C12	0.230	C6	0.242	S12	0.242	C6	0.238
D4	0.265	*V3*	0.226	S12	0.241	C6	0.241	S12	0.230
S12	0.259	S12	0.224	C12	0.237	C12	0.238	C12	0.230
Ha	0.251	C6	0.224	*V2*	0.231	*V6*	0.235	*V2*	0.221
C12	0.250	*V5*	0.217	*V6*	0.226	*V2*	0.230	D4	0.217
A4	0.245	*V6*	0.217	D4	0.220	*V3*	0.218	*V6*	0.217
V2	0.244	Ha	0.210	*V3*	0.220	D4	0.217	*V3*	0.216
V6	0.242	**A20**	0.194	**A20**	0.219	D8	0.215	D8	0.204
A20	0.242	*V2*	0.188	D8	0.214	**A20**	0.212	*V5*	0.201
V5	0.233	D8	0.180	*V5*	0.213	*CDF*	0.210	**A20**	0.197
V3	0.231	**A12**	0.178	*CDF*	0.210	*V5*	0.201	*CDF*	0.192
D8	0.231	*CDF*	0.176	**A4**	0.199	**A4**	0.198	**A12**	0.189
A8	0.214	C18	0.175	Ha	0.198	**A12**	0.190	C18	0.186
CDF	0.214	**A4**	0.175	**A12**	0.190	*An*	0.185	**A4**	0.182
An	0.209	D4	0.172	*An*	0.189	C18	0.184	S8	0.181
A12	0.208	S10	0.165	S8	0.187	S8	0.184	*An*	0.180
LG	0.203	S8	0.164	C18	0.185	**A8**	0.180	*Od*	0.173
S8	0.201	**A8**	0.158	**A8**	0.178	Ha	0.178	*LG*	0.171
C18	0.199	*V4*	0.155	*Od*	0.174	*Od*	0.175	Ha	0.166
Od	0.189	*An*	0.153	*LG*	0.164	*LG*	0.172	**A8**	0.165
A6	0.183	*LG*	0.150	S10	0.163	S10	0.168	S10	0.153
S10	0.183	*Od*	0.146	**A6**	0.155	*V4*	0.160	*V4*	0.149
V4	0.177	D6	0.138	*V4*	0.155	D6	0.144	D6	0.146
D6	0.173	**A6**	0.122	D6	0.148	**A6**	0.143	**A6**	0.133

7 Scope of the proposed method

It is important to clearly define the scope of the proposed method. As the experimental results have shown, the introduced algorithm increases watermark resistance to undeliberate[1] removal attacks[2], e.g. image compression or filtering. Nevertheless, wavelet bases adaptation is not a universal solution to all the security problems that arise in the field of image watermarking. The method will not increase robustness against desynchronization attacks, e.g. geometric attacks like cropping, scaling or rotation. The watermarking algorithm must ensure that the synchronization is regained after such an attack [10]. Please note that in our experiments, we carried out scaling attack by scaling the image down to 40% of its original size and then scaling it back to its original size, thus inverting the desynchronization. The proposed method does not also increase robustness

[1] Not exploiting knowledge of the watermark embedding scheme, watermark sequence etc.

[2] According to classification by Voloshynovskiy et al. [16].

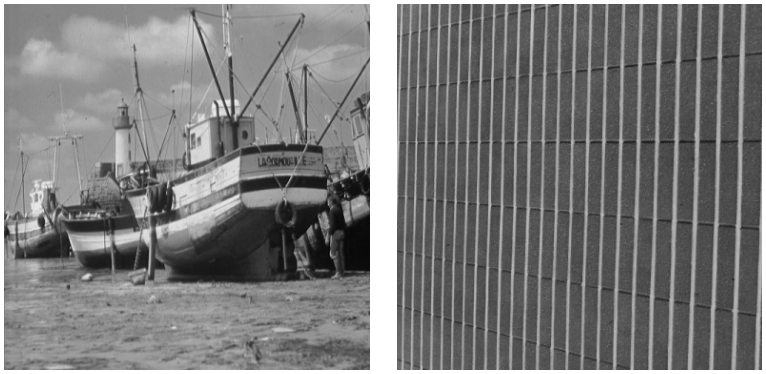

(a) Boat (b) texture

Fig. 5: Example test images.

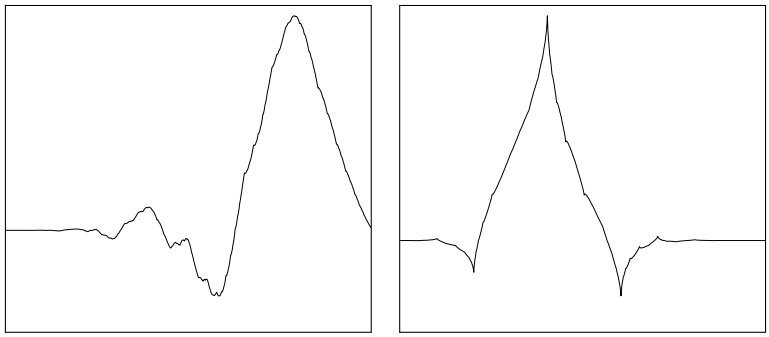

(a) Scaling function synthesized for Boat test image.

(b) Scaling function synthesized for texture test image.

Fig. 6: Adaptive scaling functions.

against protocol, coping and sensitivity attacks and it does not increase security of invertible or quasi-invertible [4] watermarking algorithms.

8 Conclusions

In this paper, the problem of improving digital watermarking effectiveness by wavelet synthesis is addressed. Genetic-based method of adapting the wavelets to the image, the watermark, the embedding algorithm and selected types of removal attacks is presented. The results of experiments that are demonstrated here, as well as the experiments which were carried out on the other test images, prove that wavelets generated using the proposed method outperform the commonly used wavelet bases in terms of robustness against attacks.

References

1. M. Antonini, M. Barlaud, P. Mathieu, and I. Daubechies. Image coding using wavelet transform. *IEEE Transactions on Image Processing*, 1:205–220, April 1992.
2. G. Cheng and J. Yang. A watermarking scheme based on two-dimensional wavelet filter parametrization. In *Fifth International Conference on Information Assurance and Security, 2009. IAS '09.*, pages 301–304, August 2009.
3. A. Cohen, I. Daubechies, and J.-C. Feauveau. Biorthogonal bases of compactly supported wavelets. *Communications on Pure and Applied Mathematics*, 45(5):485–560, June 1992.
4. S. Craver, N. Memon, B.-L. Yeo, and M.M. Yeung. Resolving rightful ownerships with invisible watermarking techniques: Limitations, attacks, and implications. *IEEE Journal on Selected Areas in Communications*, 16(4):573–586, May 1998.
5. I. Daubechies. *Ten Lectures on Wavelets*. SIAM, 1992.
6. G. Davis. Wavelet image compression construction kit. http://www.geoffdavis.net/dartmouth/wavelet/wavelet.html, 1997.
7. M. Dietze and S. Jassim. Filters ranking for DWT-domain robust digital watermarking. *EURASIP Journal on Applied Signal Processing*, 14:2093–2101, 2004.
8. Z. Q. Huang and Z. Jiang. Watermarking still images using parametrized wavelet systems. In *Image and Vision Computing*. Institute of Information Sciences and Technology, Massey University, 2003.
9. D. Le Gall and A. Tabatabai. Sub-band coding of digital images using symmetric short kernel filters and arithmetic coding techniques. In *International Conference on Acoustics, Speech, and Signal Processing, 1988. ICASSP-88.*, 1988.
10. V. Licks and R. Jordan. Geometric attacks on image watermarking systems. *IEEE Multimedia*, 12(3):68–78, 2005.
11. P. Lipiński and J. Stolarek. Digital watermarking enhancement using wavelet filter parametrization. In A. Dobnikar, U. Lotrič, and B. Šter, editors, *Adaptive and Natural Computing Algorithms (10th ICANNGA, 2011)*, volume 1, pages 330–339, 2011.
12. A. Miyazaki. A study on the best wavelet filter bank problem in the wavelet-based image watermarking. In *18th European Conference on Circuit Theory and Design, 2007. ECCTD 2007.*, pages 184–187, August 2007.
13. P. Rieder, J. Götze, J. S. Nossek, and C. S. Burrus. Parameterization of orthogonal wavelet transforms and their implementation. *IEEE Transactions on Circuits and Systems II: Analog and Digital Signal Processing*, 45(2):217–226, February 1998.
14. P. P. Vaidyanathan and P.-Q. Hoang. Lattice structures for optimal design and robust implementation of two-channel perfect-reconstruction QMF banks. *IEEE Transactions on Acoustics, Speech and Signal Processing*, 36(1):81–94, January 1988.
15. J. D. Villasenor, B. Belzer, and J. Liao. Wavelet filter evaluation for image compression. *IEEE Transactions on Image Processing*, 4(8):1053–1060, August 1995.
16. S. Voloshynovskiy, S. Pereira, T. Pun, J. J. Eggers, and J.K. Su. Attacks on digital watermarks: Classification, estimation based attacks and benchmarks. *IEEE Communications Magazine*, 39(8):118–126, August 2001.
17. Z. Wang and A. C. Bovik. A universal image quality index. *IEEE Signal Processing Letters*, 9(3):81–84, March 2002.
18. M. Yatsymirskyy. Lattice structures for synthesis and implementation of wavelet transforms. *Journal of Applied Computer Science*, 17(1):133–141, 2009.